
SEQPROFT: APPLYING LORA FINETUNING FOR SEQUENCE-ONLY PROTEIN PROPERTY PREDICTIONS

Shuo Zhang, Jian K. Liu*

School of Computer Science, University of Birmingham
szz325@student.bham.ac.uk, j.liu.22@bham.ac.uk

ABSTRACT

Protein language models (PLMs) are capable of learning the relationships between protein sequences and functions by treating amino acid sequences as textual data in a self-supervised manner. However, fine-tuning these models typically demands substantial computational resources and time, with results that may not always be optimized for specific tasks. To overcome these challenges, this study employs the LoRA method to perform end-to-end fine-tuning of the ESM-2 model specifically for protein property prediction tasks, utilizing only sequence information. Additionally, a multi-head attention mechanism is integrated into the downstream network to combine sequence features with contact map information, thereby enhancing the model's comprehension of protein sequences. Experimental results of extensive classification and regression tasks demonstrate that the fine-tuned model achieves strong performance and faster convergence across multiple regression and classification tasks.

1 Introduction

Protein, as the fundamental composing part of life, plays a vital role in the living cells [1]. Understanding protein functions is important for drug discovery, personal medical treatment, and bioengineering. With the latest developments in natural language processing, protein language models (PLMs) learn to understand the relationship between protein sequences, structures, and functions by treating amino acid sequences as text [2]. By leveraging the inherent sequentiality of protein sequences, PLMs, such as ESM-2 [3] and ProfTrans [4], learn protein evolution patterns and capture protein structure information in a self-supervised manner from a large amount of unlabeled protein sequence data. Different from PLMs that only use protein sequences, some PLMs also use protein structure information. SaProt [5] performs well in protein function prediction and mutation effect prediction tasks by using both the encoded protein 3D structure and residue sequences to train the model. Lee et al. [6] proposed to add Implicit Neural Representations (INRs) of the protein surface to enhance the ability of PLM to learn protein structure representation.

Similar to the NLP field, there are many downstream prediction tasks in the protein research field, such as protein solubility prediction and protein secondary structure classification. Pre-trained converged PLMs are usually used as feature extractors to extract high-dimensional features of protein input. This process is performed offline, that is, without gradient backpropagation. The high-dimensional features are then passed as input to the designed downstream task prediction network, which is usually composed of multi-layer perceptrons (MLPs), and the final predictions are obtained after training. Although the works mentioned above demonstrated the excellent performance of the proposed PLMs on downstream tasks in their papers, such a two-stage paradigm may lead to suboptimal and non-task-specific results, because the number of parameters of the downstream network is much smaller than that of PLMs, and the high-dimensional features cannot be transferred according to the domain of certain downstream dataset [7]. Another approach is to fully finetune PLMs for each downstream task. Obviously, this requires a lot of computing resources and is very time-consuming.

To address these challenges, Sledzieski et al. [8] introduces parameter-efficient finetuning (PEFT) technique, specifically utilizing the LoRA (Low-Rank Adaptation) [9] method, to improve PLMs in proteomics. This study focuses on two key tasks: predicting protein-protein interactions (PPIs) and determining the symmetry of homooligomer quaternary

*Correspondence author

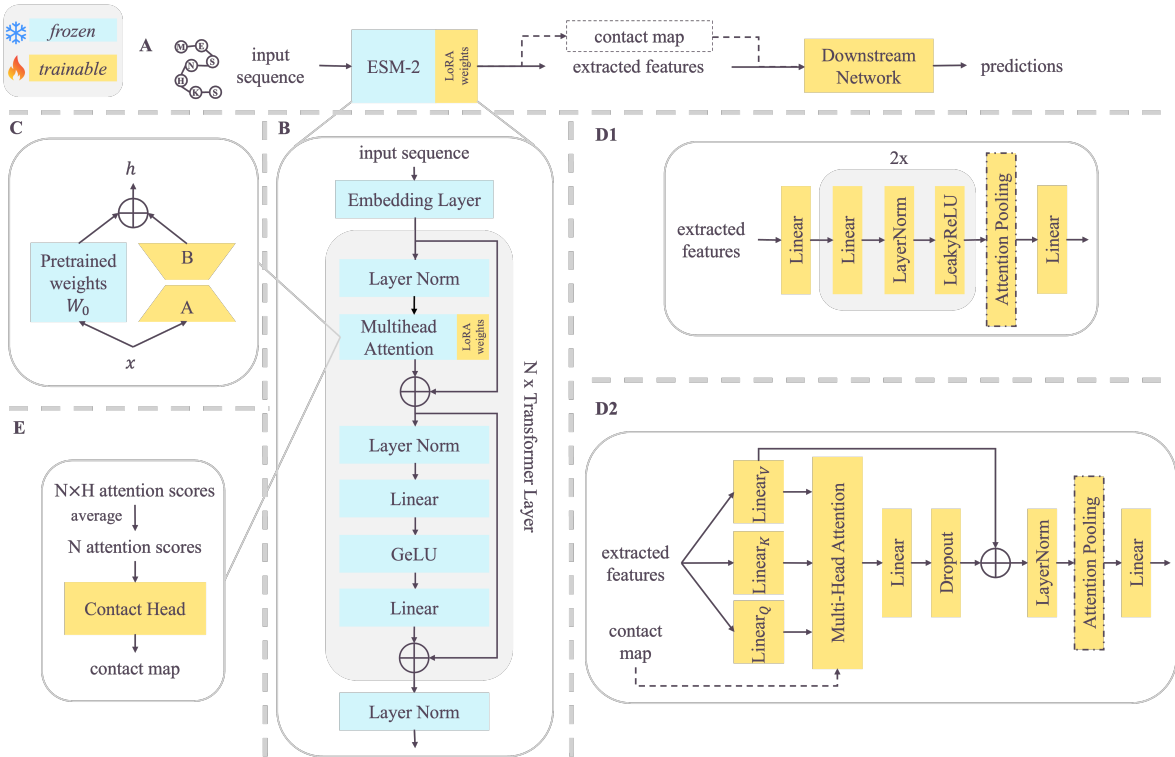


Figure 1: A: The overview of SeqProFT architecture which consists of a pretrained ESM-2 model and a downstream head. Blue blocks are frozen, and yellow blocks are trainable. B: ESM-2 mainly consists of an embedding layer, N transformer layers, and a post normalization layer. LoRA is applied on the multihead attention layer in each transformer layer of the ESM-2 model. C: In the training process, the pretrained weights are frozen, and the low-rank weights A and B are tuned. D: Different downstream networks. E: Attention scores in each transformer layer are averaged over attention heads and then passed into the trainable contact head to learn task-specific contact maps.

structures. The authors demonstrate that the PEFT approach can achieve competitive performance compared to traditional finetuning while significantly reducing memory usage and the number of required parameters. Zeng et al. [10] implement LoRA into ESM-2 [3], enabling the adaptation of evolutionary knowledge embedded in protein sequences for signal peptide prediction. Schmirler et al. [11] utilize finetuning technique compare three leading PLMs (ESM2, ProtT5 [4], Ankh [12]) on eight different protein-related tasks. In addition to lora, some works use other finetuning methods. Dickson et al. [13] highlight the challenges of annotating proteins with unknown functions and show that directly finetuning PLMs on classification tasks can significantly improve the quality of protein embeddings. The finetuned embeddings not only outperform traditional classifiers in Gene Ontology (GO) annotations but also maintain interpretability through similarity comparisons between proteins. Luo et al. [14] exploit prefix-tuning of PLMs to generate proteins tailored for specific biomedical applications, showing that multiple properties such as antimicrobial function and alpha-helix structure can be combined into single protein design.

Due to the limitations of experimental techniques such as X-ray crystallography and cryo-electron microscopy, protein structures are more difficult to determine experimentally than sequences [15]. This results in only hundreds of thousands of experimentally determined protein structures, while protein sequence data is in the billions. Most protein functional property prediction tasks only provide sequence data. Although 3D structures can be predicted using inverse folding models such as ESMFold [3], the introduced bias and time consumption cannot be ignored. Therefore, finetuning using only protein sequences is a more time-saving method and has been shown to achieve comparable performance to methods that combine structural data and other modalities [3]. Sequence-based finetuning can not only alleviate the data scarcity problem, but also exploit the rich information encoded in the sequence itself, making it a practical alternative for many tasks.

This work aims to finetune the model end-to-end to predict protein properties using only protein sequences as input. To this end, we finetune ESM-2 using LoRA while training the downstream network from scratch and compare the impact of different hyperparameters on model performance. In addition, we use the multi-head attention mechanism in

downstream head to integrate sequence features and contact maps, giving the model the ability to consider sequential and structural relationships during prediction, thereby improving its adaptability on various downstream tasks. Therefore, in addition to training the LoRA weights and the prediction head, we also allow the contact head of ESM-2 to participate in training. To verify the effectiveness of our method, we conducted experiments on multiple protein sequence-based regression and classification tasks. The experimental results show that after the introduction of LoRA, our method performs well in both accuracy and performance under different parameters and tasks.

2 Methods

Fig 1.A illustrates the workflow for predicting properties of protein sequences using a pretrained ESM-2 and LoRA weights. The frozen (blue) components are kept fixed during training, while the trainable components (yellow, like the LoRA weights) are adjustable. The ESM-2 model processes the input sequences and extracts features, which may include a contact map according to the downstream network. These features are passed along to a downstream head, which further processes them to generate task-specific predictions.

2.1 Protein Language Model ESM-2

ESM-2 is a large-scale transformer-based language model designed to predict protein structures directly from amino acid sequences (Fig 1.B). The core of the model is trained using a masked language modeling objective, where it predicts the identity of masked amino acids in protein sequences based on the surrounding context. ESM-2 scales from 8 million to 15 billion parameters. As the model’s size increases, it captures more complicated patterns in protein sequences, which correspond to the underlying biological structures.

The contact head in ESM-2 plays a crucial role in predicting residue-residue contact maps, which are essential for understanding the protein’s 3D structure. This component extracts structural information from the attention scores generated by the transformer layer, linking sequence patterns to the physical interactions between amino acids. Specifically, for a protein sequence $X = (x_1, x_2, \dots, x_L)$ of length L , the attention mechanism generates attention score $C_{ij} \in \mathbb{R}^{1 \times 1}$ that indicates the relevance of residue x_j to residue x_i :

$$C_{ij} = \text{softmax}\left(\frac{Q_i K_j^T}{\sqrt{d_k}}\right), \quad (1)$$

where $Q_i \in \mathbb{R}^{1 \times d_k}$ and $K_j \in \mathbb{R}^{1 \times d_k}$ are the query and key vectors for residue x_i and x_j , respectively, and d_k is the dimension of the key vectors. After considering the interactions of all residues, we obtain the attention scores $C \in \mathbb{R}^{L \times L}$ for sequence X .

During training, multiple layers and attention heads are used in the transformer model. In the original ESM-2 setting, the attention scores from all layers and attention heads are aggregated by stacking them and then averaging them. Considering that the stacking operation will consume a large amount of memory when introducing the batch dimension, we choose to first average the attention scores across the attention head dimension and then proceed with layer-wise stacking (Fig 1.E). The specific calculation formula is as follows:

$$\tilde{C} = \frac{1}{H_1} \sum_{h=1}^{H_1} C_h, \quad (2)$$

where H_1 is the number of attention heads, C_h is the attention scores of the h -th attention head, and $\tilde{C} \in \mathbb{R}^{L \times L}$. In biological terms, if residue i is in contact with residue j , the residue j must also be in contact with residue i . Therefore, the attention score matrix must be symmetric, i.e., $\tilde{C}_{ij} = \tilde{C}_{ji}$, which is achieved by:

$$\tilde{C}^{symm} = \tilde{C} + \tilde{C}^T. \quad (3)$$

Afterwards, we stack the symmetric attention scores from all layers:

$$\hat{C} = [\tilde{C}_1^{symm}, \tilde{C}_2^{symm}, \dots, \tilde{C}_N^{symm}], \quad (4)$$

where N is the number of transformer layers and $\hat{C} \in \mathbb{R}^{N \times L \times L}$.

To convert these attention scores into contact probabilities P (i.e., the likelihood that two residues are in contact), ESM-2 applies a linear projection that is given by:

$$P = \sigma(W_p \cdot \hat{C} + b), \quad (5)$$

where $W_p \in \mathbb{R}^{N \times 1}$ and $b \in \mathbb{R}$ are learnable weights and bias, and $\sigma(\cdot)$ is the sigmoid activation function, ensuring that the output contact map $P \in \mathbb{R}^{L \times L}$ consists of probabilities between 0 and 1.

2.2 Low-Rank Adaptation (LoRA)

LoRA injects the trainable low-rank decomposition matrices into transformer models, while freezing the pretrained weights of them. By doing this, the number of trainable parameters of downstream tasks is significantly reduced. Specifically, given the pretrained weights $W_0 \in \mathbb{R}^{d \times k}$, the accumulated gradient update ΔW is represented by two trainable low-rank decomposition matrices $A \in \mathbb{R}^{r \times k}$ and $B \in \mathbb{R}^{d \times r}$:

$$W_0 + \Delta W = W_0 + BA \tag{6}$$

, where $r \ll \min(d, k)$ is the rank of a LoRA module. A and B are initialized with random Gaussian distribution and zero, respectively. As shown in Fig 1.C, the forward propagation $h = W_0x$ after inserting LoRA is given by:

$$h = W_0x + \Delta x = W_0x + BAx. \tag{7}$$

In addition, ΔWx is scaled by $\frac{\alpha}{r}$ for stable training, where α is a constant hyperparameter. Unless otherwise specified, the rank r and scale factor α are all set to 32 in this work.

2.3 Downstream Networks

The ESM-2 extracted high-dimensional features are passed into downstream networks for task-specific finetuning. All parameters in downstream nets are trainable. We designed 3 types of downstream networks.

2.3.1 Simple MLP Head

The simple MLP head (SMH) shown in Fig 1.D1 consists of one linear layer, 2 feedforward blocks, one attention pooling layer, and the final prediction layer. Similar to [16], the attention pooling layer aggregates residue-level features into protein-level features. Given hidden feature $X \in \mathbb{R}^{L \times dk}$, we first calculate the attention score S by:

$$S = Dropout(Softmax(\frac{W_Q(W_K X^T)^T}{\sqrt{d_l}})) \in \mathbb{R}^{H_2 \times L}, \tag{8}$$

where d_l is the latent dimension and H_2 is the number of attention heads. $W_Q \in \mathbb{R}^{H_2 \times d_l}$ and $W_K \in \mathbb{R}^{H_2 \times d_l \times dk}$ are learnable weights. Then the hidden feature X is weighted and aggregated over all the residues in the sequence by attention score S to get $X_O \in \mathbb{R}^{H_2 \times d_l}$, which is given by formula 9, where $W_V \in \mathbb{R}^{H_2 \times d_l \times dk}$. Finally, as shown in formula 10, the pooled hidden feature $X_P \in \mathbb{R}^{d_k}$ is calculated by matrix-multiplying X_O with $W_O \in \mathbb{R}^{d_k \times H_2 \times d_l}$ to aggregate features from all attention heads.

$$X_O = S(W_V X^T)^T \tag{9}$$

$$X_P = W_O(X_O)^T \tag{10}$$

2.3.2 Multihead Attention Head

The prediction of protein property is a complex task, which requires considering the interactions and associations between residues. With the aim to capture the implicit relationship and improve the prediction accuracy, we utilize the multihead attention mechanism [17] to obtain the attention distributions on different sub-spaces of input protein sequence. Each head of the multihead attention mechanism learns similarity weights between residues independently. In our Multihead Attention Head (MAH) (Fig 1.D2), the extracted features are firstly fed into 3 linear projection layers to generate query, key, and value variables, which then interact with each other in the multihead attention layer. After several other layers similar to BERT [18], the hidden features are passed into the attention pooling layer and the final prediction layer for property prediction.

2.3.3 Contact Map Enhanced Multihead Attention Head

The protein structure is a determining factor of the protein property. In our contact map enhanced multihead attention head (CM-MAH), we introduce the contact map as attention weights to represent the spatial relationship between residues. Therefore, the attention mechanism is given by:

$$Attention(Q, K, V, P) = softmax(\frac{QK^T P}{\sqrt{d_{head}}})V, \tag{11}$$

where d_{head} is the feature dimension of downstream head. In formula 11, the original attention weight is further weighted by the learned contact map to allow the model to focus more on residue pairs that actually have physical contact. The other layers of CM-MAH is the same as MAH, as shown in Fig 1.D2.

Table 1: Summary of Downstream Datasets

Datasets	Train samples	Test samples	Task	Metric
EC	15551	1919	sequence-level multi-label classification	F1-max
GO	29902	3416	sequence-level multi-label classification	F1-max
Fold	12312	family / fold / superfamily 1272 / 718 / 1254	sequence-level multi-class classification	Accuracy
SS	10792	20	token-level multi-class classification	Accuracy
Loc	6622	1842	sequence-level multi-class classification	Accuracy
HumanCell	5792	1366	sequence-level regression	Spearman’s ρ
GB1	6988	1745	sequence-level regression	Spearman’s ρ
FLU	21446	27217	sequence-level regression	Spearman’s ρ
eSOL	2363	782	sequence-level regression	R^2

3 Experimental Design

3.1 Downstream tasks

We select nine downstream tasks that cover various levels of protein function and property predictions, such as solubility prediction, secondary structure prediction, and fold classification. Each task is designed to assess the model’s performance across different biological functions and structural attributes, providing a thorough evaluation of protein characteristics. Tab. 1 summarizes the statistics of these nine datasets and their subsets.

Enzyme Commission number prediction (EC) involves predicting the Enzyme Commission numbers that classify enzymes based on the chemical reactions they catalyze. Each protein sequence can belong to multiple classes out of a total 538. Accurate EC number predictions are essential for understanding enzyme functions and their roles in metabolic pathways.

Gene Ontology term prediction (GO) focuses on predicting Gene Ontology terms, which provide a standardized representation of gene and gene product attributes across species. This classification task includes three subsets: Biological Process (BP) with 1,943 classes, Cellular Component (CC) with 320 classes, and Molecular Function (MF) with 489 classes. Predicting GO term is vital for annotating protein functions and understanding their biological roles.

Fold Class prediction (Fold) aims to classify protein sequences into one of 1,195 known folds [19], which is critical for inferring evolutionary relationships and understanding how protein sequences relate to their structures. This dataset contains three test sets: family, fold, and superfamily. Unless otherwise specified, the experimental results presented are the average scores of these three test sets.

Secondary Structure prediction (SS) involves predicting the 3-class secondary structure of each residue in a protein chain [20]. This task is fundamental for protein structure determination and provides insights into protein folding and stability. We use CASP12 as test set.

Sub-cellular Localization prediction (Loc) predicts the sub-cellular localization of proteins into 10 different classes, which is essential for understanding their functional context within a cell. Accurate localization predictions help clarify protein functions and interactions in various cellular compartments.

Thermostability prediction (HumanCell) is a regression task that predicts the thermostability of each protein sequence. Understanding protein thermostability is important for biotechnology applications and designing proteins with enhanced stability for therapeutic uses. Due to limited computing resources, we choose the smallest subset, HumanCell, from the original paper [21].

GB1 Fitness prediction (GB1), proposed in [21], is a regression task where the model learns the epistatic interactions between mutations. This is vital for engineering proteins with desired properties.

Fluorescence Landscape Prediction (FLU), introduced in [22], is another regression task. The dataset is partitioned based on the Hamming distances between the parent green fluorescent protein (GFP) and its mutants. The training set includes mutants with a Hamming distance of 3 from the parent GFP, while the test set comprises more distant variants with four or more mutants. Predicting this landscape helps identify mutations that enhance or impair protein performance.

Solubility prediction (eSOL) aims to predict protein solubility, which is a key factor in their expression, purification, and functionality. The eSOL dataset was first introduced in [23]. This regression task is essential for understanding diseases caused by protein aggregation.

For EC, GO and Fold, we use the dataset splits from GearNet [24]. For SS, Loc, and FLU, we follow the dataset splits provided in Ankh [12]. For HumanCell and GB1, we adopt the dataset splits from FLIP [21], and for eSOL, we adopt the splits from [25].

3.2 Loss Functions and Evaluation Metrics

We select different loss functions and evaluation metrics for different tasks.

3.2.1 Classification Tasks

For multi-label classification tasks EC and GO, we use multi-label binary cross entropy as loss function, which is given by:

$$ML-BCE(y, p) = -\frac{1}{C_{task}} \sum_{i=1}^{C_{task}} [y_i \cdot \log(p_i) + (1 - y_i) \cdot \log(1 - p_i)], \quad (12)$$

where C_{task} is the number of classes, y_i is the ground truth of the i -th category, and p_i is the predicted probabilities of the i -th category.

For multi-class classification tasks Fold, Loc, and SS, we use cross entropy loss function:

$$CE(y, p) = -\sum_{i=1}^{C_{task}} y_i \cdot \log(p_i). \quad (13)$$

3.2.2 Regression Tasks

For regression tasks HumanCell, GB1, FLU, and eSOL, we use the mean squared error as loss function:

$$MSE = \frac{1}{N_{sample}} \sum_i^{N_{sample}} (y_i - p_i)^2, \quad (14)$$

where N_{sample} is the number of input samples.

For a fair comparison, we used the same evaluation metrics as the baselines: F1-max for EC and GO, accuracy for Fold, SS, and Loc, Spearman’s ρ for HumanCell, GB1, and FLU, and R^2 for eSOL. Tab. 2 provides the formula of each metric.

Table 2: Formula of evaluation metrics. d_i is the difference in rank between the i -th observation in the two variables.

Metric	Formula
F1-max	$\frac{2 \times TP}{2 \times TP + FP + FN}$
Accuracy	$\frac{TP + TN}{TP + TN + FP + FN}$
Spearman’s ρ	$\rho = 1 - \frac{6 \sum d_i^2}{N_{sample}(N_{sample}^2 - 1)}$
R^2	$R^2 = 1 - \frac{\sum_{i=1}^{N_{sample}} (y_i - p_i)^2}{\sum_{i=1}^{N_{sample}} (y_i - \bar{y})^2}$

3.3 Training Setup

To balance computing resources and performance, we select three ESM-2 models with different sizes for extracting high-dimensional features: 35M, 150M, and 650M. As mentioned earlier, we use three different prediction heads to assess the performance differences of various architectures in processing protein sequence features. SMH serves as the basic baseline model, MAH incorporates multihead attention, and CM-MAH introduces learnable structural information. By comparing the outcomes of these prediction heads, we can analyze how different tasks require specific model architectures.

Table 4: Results of with and without LoRA fine-tuning on the test sets of all tasks. 'w/': with LoRA finetuning. 'w/o': without LoRA finetuning. ' Δ ': performance improvement after using LoRA finetuning. '%': percentage increase.

Size	Settings	EC	GO-BP	GO-CC	GO-MF	Fold	SS	Loc	FLU	HumanCell	GB1	eSOL
35M	w/o	0.732	0.391	0.522	0.486	57.7	74.5	75.0	0.621	0.671	0.811	0.488
	w/	0.798	0.411	0.571	0.500	61.9	75.2	76.0	0.684	0.682	0.942	0.508
	Δ	+0.066	+0.02	+0.049	+0.014	+4.2	+0.7	+1.0	+0.063	+0.011	+0.131	+0.02
	%	9.02%	5.12%	9.39%	2.88%	7.28%	0.94%	1.33%	10.14%	1.64%	16.15%	4.10%
150M	w/o	0.807	0.419	0.586	0.495	63.1	78.8	78.1	0.636	0.683	0.900	0.505
	w/	0.853	0.441	0.636	0.527	64.6	79.4	79.9	0.679	0.695	0.957	0.493
	Δ	+0.046	+0.022	+0.05	+0.032	+1.5	+0.6	+1.7	+0.043	+0.012	+0.057	-0.012
	%	5.70%	5.25%	8.53%	6.46%	2.38%	0.76%	2.18%	6.76%	1.76%	6.33%	-2.38%
650M	w/o	0.848	0.428	0.617	0.507	64.6	81.8	80.6	0.633	0.690	0.888	0.523
	w/	0.887	0.460	0.674	0.513	68.2	82.5	83.0	0.684	0.708	0.958	0.546
	Δ	+0.039	+0.032	+0.057	+0.006	+3.6	+0.7	+2.4	+0.051	+0.018	+0.07	+0.023
	%	4.60%	7.48%	9.24%	1.18%	5.57%	0.86%	2.98%	8.06%	2.61%	7.88%	4.40%

All the experiments were run on a single A100 40G GPU. We performed a hyperparameter search to find the optimal learning rate from the following options: [5e-6, 1e-6, 5e-5, 1e-5, 5e-4, 1e-4]. For each learning rate, the model was run for 3 epochs, and we chose the one that gave the best performance. The final learning rates and total epochs for each dataset are summarized in Tab. 3.

Table 3: Learning rate and total epochs.

dataset	lr	epoch
EC	1e-4	20
GO-BP	1e-4	20
GO-MF	1e-4	20
GO-CC	1e-4	20
Fold	5e-4	10
SS	1e-4	20
Loc	5e-4	10
FLU	1e-4	20
HumanCell	5e-4	10
GB1	5e-5	50
eSOL	5e-4	10

We applied gradient accumulation during training and updated the weights every 16 samples. The code was implemented using the PyTorch framework and the Hugging Face transformers library [26] to load and finetune the ESM-2 model. All models are trained with mixed precision, and to ensure reproducibility, all experiments are conducted with a fixed random seed. To evaluate the adaptability of LoRA finetuning across models of different sizes and tasks, we design a comprehensive set of experiments to ensure the results are generalized and representative. Following [8] and [11], we set the alpha value to 32 and enumerate the rank value in [1, 2, 4, 8, 16, 32]. The weight matrices for low-rank decomposition include the query, key, value, and other linear layers in the attention layer of ESM-2.

4 Results and Discussion

4.1 LoRA enables stronger adaptation on downstream tasks

We evaluated the effectiveness of LoRA finetuning across 11 datasets, using ESM-2 models with three different parameter sizes (35M, 150M, and 650M) as initial weights, and CM-MAH as the downstream task head. Tab. 4 presents the performance of each model on various tasks and quantifies the performance gains (Δ) after applying LoRA

finetuning. Models finetuned with LoRA (denoted as 'w/') demonstrate significant improvements across all tasks and model sizes compared to those without LoRA finetuning (denoted as 'w/o').

For the 35M model, LoRA finetuning consistently enhances model performance, showing substantial gains in most tasks, particularly in EC (+9.02%), Fold (+7.28%), and FLU (+10.14%). The 150M model exhibits higher baseline performance, and with LoRA finetuning, the maximum improvement reaches 8.53%. The 650M model, with the largest parameter count, delivers the best overall results, achieving the highest gains in tasks such as GO-BP (+7.48%), Loc (+2.98%), HumanCell (+2.61%), and eSOL (+4.4%). However, for the eSOL solubility prediction task, the 150M model's performance slightly decreased (-2.38%), suggesting potential overfitting at this scale.

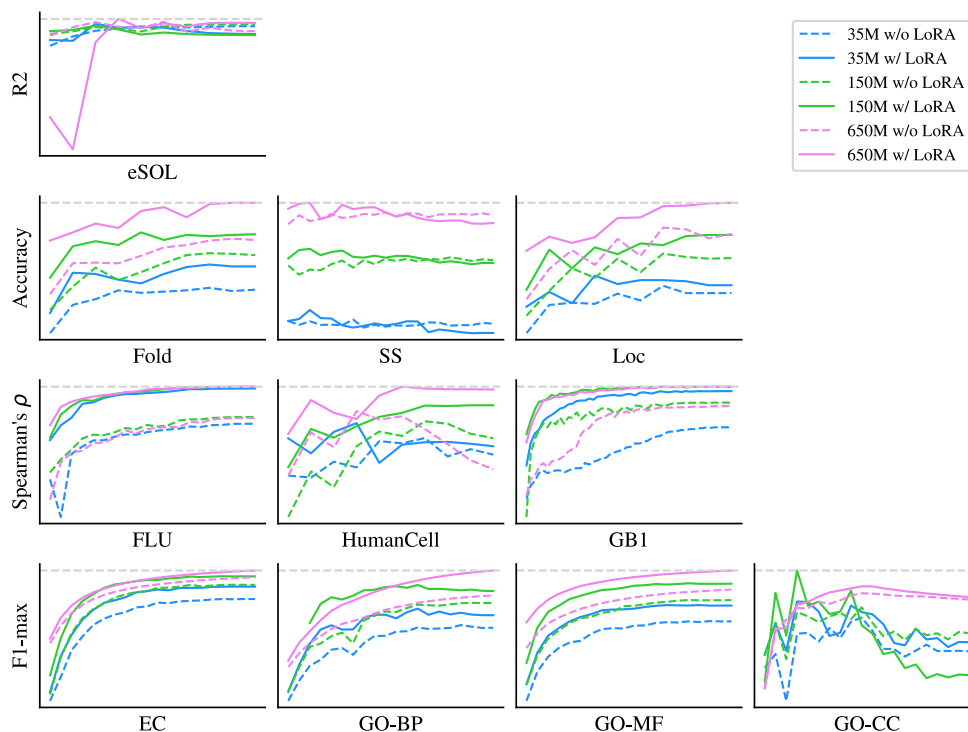


Figure 2: The performance of LoRA finetuning with different ESM-2 sizes at different training steps.

Fig. 2 illustrates the performance of ESM-2 models of various sizes with LoRA finetuning across different training steps. In several tasks, models using LoRA finetuning (solid lines) exhibit faster convergence compared to those without it (dashed lines). Models with fewer parameters, such as the 35M and 150M, achieve a converged state more quickly during training. In contrast, the 650M model, due to its larger parameter size, requires more time to reach a comparable level of convergence.

Interestingly, in tasks like EC, GO, Fold, and FLU, the performance of the 150M model with LoRA finetuning surpasses that of the 650M model without LoRA finetuning. This finding indicates that smaller models, when finetuned with LoRA, can overcome the limitations of fewer parameters and, in some cases, perform on par with or better than larger models. The primary advantage of LoRA finetuning lies in its ability to enhance model performance by modifying only a few additional parameters, while keeping most of the original model parameters frozen. This approach allows the model to better adapt to the specific data distribution and features of a given task, significantly enhancing the adaptability of smaller models. This is particularly beneficial when the available data is limited, as large models are prone to overfitting due to their extensive parameter count. We recommend employing LoRA finetuning in resource-constrained protein research applications, such as online services and mobile devices, rather than solely focusing on increasing model size. This method not only maintains strong performance in environments with limited resources but also effectively mitigates the risk of overfitting.

Table 6: Results of applying LoRA to different transformer weights.

Module	EC		Fold		Loc		FLU		HumanCell		GB1	
	-	+ W_d	-	+ W_d	-	+ W_d	-	+ W_d	-	+ W_d	-	+ W_d
W_Q	0.759	0.787	60.5	61.4	75.1	75.7	0.669	0.681	0.683	0.687	0.905	0.938
W_K	0.766	0.787	60.6	61.3	75.5	76.4	0.672	0.680	0.682	0.683	0.901	0.943
W_V	0.762	0.784	62.0	60.8	75.8	76.1	0.669	0.680	0.695	0.688	0.912	0.941
W_Q, W_K	0.763	0.789	61.4	61.7	75.1	76.1	0.677	0.680	0.678	0.685	0.918	0.940
W_K, W_V	0.774	0.789	61.2	61.1	75.7	76.4	0.677	0.679	0.687	0.685	0.924	0.942
W_Q, W_V	0.770	0.788	61.3	61.7	75.7	76.2	0.674	0.679	0.688	0.684	0.923	0.940
W_Q, W_K, W_V	0.775	0.798	62.5	61.9	75.8	75.7	0.677	0.684	0.684	0.682	0.930	0.942

4.2 Could contact information bring positive results?

Table 5: Performance of different downstream heads. ESM-2-35M is used.

Settings	EC	Fold	FLU	GB1
SMH	0.771	58.8	0.683	0.942
MAH	0.785	59.4	0.679	0.938
CM-MAH	0.798	61.9	0.684	0.942

To investigate whether contact information between protein amino acids can improve prediction accuracy, we designed the experiment presented in Tab. 5. We finetuned the ESM-2-35M model using LoRA and applied three different downstream task prediction heads across four tasks. Among these tasks, EC and Fold are classification tasks, while FLU and GB1 are regression tasks.

When introducing the multi-head attention mechanism, the MAH showed slight improvements in the EC and Fold tasks compared to the SMH which stacks several linear layers. Specifically, MAH improved performance by 0.014 on the EC task and by 0.6 on the Fold task. However, its performance on the regression tasks FLU and GB1 slightly declined, both by 0.004.

More notable changes were observed with CM-MAH. In CM-MAH, we utilized contact information obtained from retraining the contact head of the ESM-2 model as the weight matrix for the multi-head attention. This adjustment led to significant performance improvements. For the EC task, CM-MAH improved by 0.027 compared to SMH and by 0.013 compared to MAH. In the Fold task, CM-MAH showed an improvement of 3.1 over SMH and 2.5 over MAH. In contrast, for the regression tasks, the performance of CM-MAH was almost the same as that of SMH and MAH, with a slight edge in the FLU task and matching SMH in the GB1 task.

These results suggest that training the contact head and incorporating contact information during finetuning enhances the model’s representation ability in classification tasks. However, this approach offers limited improvements for regression tasks. This difference could be due to the distinct feature requirements of classification and regression tasks. Classification tasks often depend on both local and global patterns within protein structures, which contact maps can provide effectively. In contrast, regression tasks are more focused on predicting continuous values and may rely more heavily on global sequence features rather than specific contact information. Although contact maps can enrich structural representation, this information may not directly contribute to performance enhancement in regression tasks. Future research could explore optimizing the use of contact maps or integrating them with other features to further improve model performance across various tasks.

4.3 Analyzing Transformer Module Importance and Effect of Rank in LoRA Finetuning

Table 7: There is no direct linear relationship between rank and the effect of LoRA finetuning.

rank	EC	Fold	Loc	FLU	HumanCell	GB1
1	0.779	61.9	75.5	0.680	0.687	0.944
2	0.790	62.4	75.8	0.681	0.682	0.943
4	0.787	61.1	75.8	0.682	0.686	0.945
8	0.789	61.8	75.9	0.680	0.685	0.945
16	0.791	61.5	76.2	0.680	0.684	0.941
32	0.798	61.9	75.7	0.684	0.682	0.942

We designed a series of experiments to explore whether a particular parameter combination for LoRA yields superior performance across different downstream tasks. We selected three classification tasks (EC, Fold, and Loc) and three regression tasks (FLU, HumanCell, and GB1).

Firstly, Tab. 6 illustrates the effects of applying LoRA to various Transformer weight matrices (query, key, value, and other dense layers). Our results indicate that, for classification tasks, the best performance is achieved when LoRA is applied to all three matrices (W_Q, W_K, W_V). This configuration consistently outperforms other combinations. In contrast, for regression tasks, no clear pattern emerges regarding the optimal parameter combination, suggesting variability in performance across different settings.

When LoRA is applied to the other dense layers, most combinations show varying degrees of performance improvement. However, there are instances where performance decreases, such as in the Fold dataset with the W_Q, W_K, W_V combination.

Secondly, Tab. 7 presents the impact of different ranks on model performance. No distinct relationship between rank and model performance is observed across the six tasks. Notably, larger ranks, which correspond to more trainable parameters, do not necessarily result in better results. For instance, on the HumanCell dataset, a rank of 1 achieves the highest Spearman’s ρ , although differences between maximum and other results are relatively small. This observation aligns with previous findings in [9], which suggest that smaller ranks are sufficient.

4.4 Comparison with the State-Of-The-Art Methods

Table 8: The results of compared methods using sequence only or additional data features in EC, GO, and Fold. SeqProFT version: ESM-2-650M, CM-MAH, and with LoRA fine-tune.

Methods	Seq. Only	EC	GO			Fold
			BP	MF	CC	
DeepFRI [27]	x	0.631	0.399	0.465	0.46	36.4
GearNet [24]	x	0.730	0.356	0.503	0.414	55.4
GearNet-MC [24]	x	0.874	0.490	0.654	0.488	78.2
ProtST-ESM-2 [28]	x	0.878	0.482	0.668	0.487	-
ESM-1B-GearNet [29]	x	0.883	0.491	0.677	0.501	-
ESM-2-GearNet [30]	x	0.897	0.514	0.683	0.505	-
ProteinINR [6]	x	0.896	0.518	0.683	0.504	50.8
CNN [31]	✓	0.545	0.244	0.354	0.287	26.0
ESM-2-RS [32]	✓	0.817	0.519	0.678	0.485	-
ESM-1B (from [28])	✓	0.869	0.452	0.659	0.477	-
ESM-2 (from [28])	✓	0.874	0.472	0.662	0.472	-
SeqProFT	✓	0.887	0.460	0.674	0.513	68.2

Tab. 8 and Tab. 9 show the comparison of our model with several state-of-the-art (SOTA) models. In this analysis, SeqProFT with ESM-2-650M and CM-MAH is finetuned using LoRA (r=32, alpha=32). The models in [27], [24], [29], [30], and [6] utilize additional protein structure data, while [28] incorporates biomedical text data. All other methods in the tables use only protein sequence data for model training. Our approach outperforms other sequence-only methods

on the EC, GO-CC, Fold, HumanCell, GB1, and eSOL datasets. It is important to note that ESM-2 (from [11]) is fully finetuned and Ankh [12] has 1.5 billion parameters.

Table 9: The results of compared methods using sequence only in the rest of tasks. SeqProFT version: ESM-2-650M, CM-MAH, and with LoRA finetune.

Methods	SS	Loc	FLU	HumanCell	GB1	eSOL
ESM-2 (from [12])	82.3	81.8	0.48	-	0.82	-
Ankh [12]	83.8	83.2	0.62	-	0.84	-
ESM-2 (from [11])	85.5	63.8	0.688	-	-	-
ESM-1B (from [28])	-	78.1	0.679	0.669	-	-
ESM-2 (from [28])	-	78.7	0.677	0.672	-	-
NetSolP [33]	-	-	-	-	-	0.449
GraphSOL [16]	-	-	-	-	-	0.501
HybridGCN [25]	-	-	-	-	-	0.510
GATSol [34]	-	-	-	-	-	0.517
SeqProFT	82.5	83.0	0.684	0.708	0.958	0.546

While our method does not fully match the performance of models using additional modalities, it demonstrates significant comparability. This indicates that SeqProFT can be a valuable option for predicting protein properties in datasets lacking structural information and only using sequence as inputs. Furthermore, as shown in Fig. 2, the test set performance on many datasets continues to improve, but due to limited computational resources, we could not conduct further training. We believe that with extended training, SeqProFT would achieve even better results on datasets such as EC and GO-BP.

5 Conclusion

In this study, we propose SeqProFT, a LoRA finetuning based framework for sequence-only protein functional property prediction. Through end-to-end finetuning of the ESM-2 model, combined with a multi-head attention mechanism and contact map prediction, SeqProFT can effectively learn the local and global features of protein sequences, thereby enhancing the adaptability to various downstream tasks. We conducted extensive experiments on 11 downstream tasks to systematically analyze its effectiveness and potential. The results show that in classification and regression tasks, SeqProFT performs excellently in terms of model performance and convergence speed. In some tasks, different parameter configurations and module selections of LoRA have a significant impact on model performance, so we recommend adjusting the finetuning strategy according to specific downstream tasks. In addition, despite the overall excellent performance of LoRA finetuning, increasing model complexity does not always bring improvements, especially in regression tasks, where larger PLMs are not always the best choice. Therefore, we recommend designing customized algorithms for specific tasks and delving into the intrinsic properties of the dataset. Finally, for small laboratories with limited resources or online platforms, LoRA finetuning of small size PLMs can be an effective alternative to large models.

References

- [1] Bruch Alberts, Rebecca Heald, Alexander Johnson, David Morgan, Martin Raff, Keith Roberts, Peter Walter, John Wilson, and Tim Hunt. *Protein Function*, chapter 3, pages 140–179. W. W. Norton & Company, 2022.
- [2] Ali Madani, Ben Krause, Eric R. Greene, Subu Subramanian, Benjamin P. Mohr, James M. Holton, Jose Luis Olmos, Caiming Xiong, Zachary Z. Sun, Richard Socher, James S. Fraser, and Nikhil Naik. Large language models generate functional protein sequences across diverse families. *Nature Biotechnology*, 41(8):1099–1106, 2023.
- [3] Zeming Lin, Halil Akin, Roshan Rao, Brian Hie, Zhongkai Zhu, Wenting Lu, Nikita Smetanin, Robert Verkuil, Ori Kabeli, Yaniv Shmueli, et al. Evolutionary-scale prediction of atomic-level protein structure with a language model. *Science*, 379(6637):1123–1130, 2023.
- [4] Ahmed Elnaggar, Michael Heinzinger, Christian Dallago, Ghalia Rehawi, Wang Yu, Llion Jones, Tom Gibbs, Tamas Feher, Christoph Angerer, Martin Steinegger, Debsindhu Bhowmik, and Burkhard Rost. Prottrans: Towards cracking the language of lifes code through self-supervised deep learning and high performance computing. *IEEE Transactions on Pattern Analysis and Machine Intelligence*, pages 1–1, 2021.

- [5] Jin Su, Chenchen Han, Yuyang Zhou, Junjie Shan, Xibin Zhou, and Fajie Yuan. Saprot: Protein language modeling with structure-aware vocabulary. In *The Twelfth International Conference on Learning Representations*, 2024.
- [6] Youhan Lee, Hasun Yu, Jaemyung Lee, and Jaehoon Kim. Pre-training sequence, structure, and surface features for comprehensive protein representation learning. In *The Twelfth International Conference on Learning Representations*, 2024.
- [7] Junxian He, Chunting Zhou, Xuezhe Ma, Taylor Berg-Kirkpatrick, and Graham Neubig. Towards a unified view of parameter-efficient transfer learning. In *International Conference on Learning Representations*, 2022.
- [8] Samuel Sledzieski, Meghana Kshirsagar, Minkyung Baek, Rahul Dodhia, Juan Lavista Ferres, and Bonnie Berger. Democratizing protein language models with parameter-efficient fine-tuning. *Proceedings of the National Academy of Sciences*, 121(26), 2024.
- [9] Edward J Hu, Yelong Shen, Phillip Wallis, Zeyuan Allen-Zhu, Yanzhi Li, Shean Wang, Lu Wang, and Weizhu Chen. LoRA: Low-rank adaptation of large language models. In *International Conference on Learning Representations*, 2022.
- [10] Shuai Zeng, Duolin Wang, Lei Jiang, and Dong Xu. Parameter-efficient fine-tuning on large protein language models improves signal peptide prediction. *Genome Research*, page gr.279132.124, 2024.
- [11] Robert Schmirler, Michael Heinzinger, and Burkhard Rost. Fine-tuning protein language models boosts predictions across diverse tasks. *bioRxiv*, 2023.
- [12] Ahmed Elnaggar, Hazem Essam, Wafaa Salah-Eldin, Walid Moustafa, Mohamed Elkerdawy, Charlotte Rochereau, and Burkhard Rost. Ankh: Optimized protein language model unlocks general-purpose modelling. *arXiv preprint arXiv:2301.06568*, 2023.
- [13] Andrew Dickson and Mohammad R K Mofrad. Fine-tuning protein embeddings for functional similarity evaluation. *Bioinformatics*, 40(8), 2024.
- [14] Jiawei Luo, Xianliang Liu, Jiahao Li, Qingcai Chen, and Junjie Chen. Flexible and controllable protein design by prefix-tuning protein language models. *bioRxiv*, 2023.
- [15] Eugene Y.D. Chua, Joshua H. Mendez, Micah Rapp, Serban L. Ilca, Yong Zi Tan, Kashyap Maruthi, Huihui Kuang, Christina M. Zimanyi, Anchi Cheng, Edward T. Eng, Alex J. Noble, Clinton S. Potter, and Bridget Carragher. Better, faster, cheaper: Recent advances in cryo-electron microscopy. *Annual Review of Biochemistry*, 91(1):1–32, 2022.
- [16] Jianwen Chen, Shuangjia Zheng, Huiying Zhao, and Yuedong Yang. Structure-aware protein solubility prediction from sequence through graph convolutional network and predicted contact map. *Journal of cheminformatics*, 13(1):1–10, 2021.
- [17] Ashish Vaswani, Noam Shazeer, Niki Parmar, Jakob Uszkoreit, Llion Jones, Aidan N Gomez, Łukasz Kaiser, and Illia Polosukhin. Attention is all you need. In *Advances in Neural Information Processing Systems*, volume 30. Curran Associates, Inc., 2017.
- [18] Jacob Devlin, Ming-Wei Chang, Kenton Lee, and Kristina Toutanova. BERT: Pre-training of deep bidirectional transformers for language understanding. In *Proceedings of the 2019 Conference of the North American Chapter of the Association for Computational Linguistics: Human Language Technologies, Volume 1 (Long and Short Papers)*, pages 4171–4186. Association for Computational Linguistics, 2019.
- [19] Jie Hou, Badri Adhikari, and Jianlin Cheng. DeepSF: deep convolutional neural network for mapping protein sequences to folds. *Bioinformatics*, 34(8):1295–1303, 2017.
- [20] Michael Schantz Klausen, Martin Closter Jespersen, Henrik Nielsen, Kamilla Kjærgaard Jensen, Vanessa Isabell Jurtz, Casper Kaae Sønderby, Morten Otto Alexander Sommer, Ole Winther, Morten Nielsen, Bent Petersen, and Paolo Marcatili. Netsurfp-2.0: Improved prediction of protein structural features by integrated deep learning. *Proteins: Structure, Function, and Bioinformatics*, 87(6):520–527, 2019.
- [21] Christian Dallago, Jody Mou, Jody Mou, Kadina Johnston, Bruce Wittmann, Nicholas Bhattacharya, Samuel Goldman, Ali Madani, and Kevin Yang. Flip: Benchmark tasks in fitness landscape inference for proteins. In J. Vanschoren and S. Yeung, editors, *Proceedings of the Neural Information Processing Systems Track on Datasets and Benchmarks*, volume 1, 2021.
- [22] Roshan Rao, Nicholas Bhattacharya, Neil Thomas, Yan Duan, Xi Chen, John Canny, Pieter Abbeel, and Yun S Song. Evaluating protein transfer learning with tape. In *Advances in Neural Information Processing Systems*, 2019.
- [23] Tatsuya Niwa, Bei-Wen Ying, Katsuyo Saito, WenZhen Jin, Shoji Takada, Takuya Ueda, and Hideki Taguchi. Bimodal protein solubility distribution revealed by an aggregation analysis of the entire ensemble of *Escherichia coli* proteins. *Proceedings of the National Academy of Sciences*, 106(11):4201–4206, 2009.

- [24] Zuobai Zhang, Minghao Xu, Arian Rokkum Jamasb, Vijil Chenthamarakshan, Aurelie Lozano, Payel Das, and Jian Tang. Protein representation learning by geometric structure pretraining. In *The Eleventh International Conference on Learning Representations*, 2023.
- [25] Long Chen, Rining Wu, Feixiang Zhou, Huifeng Zhang, and Jian K. Liu. Hybridgen for protein solubility prediction with adaptive weighting of multiple features. *Journal of Cheminformatics*, 15(1), 2023.
- [26] Thomas Wolf, Lysandre Debut, Victor Sanh, Julien Chaumond, Clement Delangue, Anthony Moi, Pierric Cistac, Tim Rault, Rémi Louf, Morgan Funtowicz, Joe Davison, Sam Shleifer, Patrick von Platen, Clara Ma, Yacine Jernite, Julien Plu, Canwen Xu, Teven Le Scao, Sylvain Gugger, Mariama Drame, Quentin Lhoest, and Alexander M. Rush. Transformers: State-of-the-art natural language processing. In *Proceedings of the 2020 Conference on Empirical Methods in Natural Language Processing: System Demonstrations*, pages 38–45, Online, 2020. Association for Computational Linguistics.
- [27] Vladimir Gligorijević, P. Douglas Renfrew, Tomasz Kosciolk, Julia Koehler Leman, Daniel Berenberg, Tommi Vatanen, Chris Chandler, Bryn C. Taylor, Ian M. Fisk, Hera Vlamakis, Ramnik J. Xavier, Rob Knight, Kyunghyun Cho, and Richard Bonneau. Structure-based protein function prediction using graph convolutional networks. *Nature Communications*, 12(1), 2021.
- [28] Minghao Xu, Xinyu Yuan, Santiago Miret, and Jian Tang. Protst: Multi-modality learning of protein sequences and biomedical texts. *arXiv preprint arXiv:2301.12040*, 2023.
- [29] Zuobai Zhang, Minghao Xu, Aurelie Lozano, Vijil Chenthamarakshan, Payel Das, and Jian Tang. Enhancing protein language model with structure-based encoder and pre-training. In *ICLR 2023 - Machine Learning for Drug Discovery workshop*, 2023.
- [30] Zuobai Zhang, Chuanrui Wang, Minghao Xu, Vijil Chenthamarakshan, Aurelie Lozano, Payel Das, and Jian Tang. A systematic study of joint representation learning on protein sequences and structures. *arXiv preprint arXiv:2303.06275*, 2023.
- [31] Amir Shanehsazzadeh, David Belanger, and David Dohan. Is transfer learning necessary for protein landscape prediction?, 2020.
- [32] Zuobai Zhang, Jiarui Lu, Vijil Chenthamarakshan, Aurélie Lozano, Payel Das, and Jian Tang. Structure-informed protein language model, 2024.
- [33] Vineet Thumulari, Hannah-Marie Martiny, Jose J Almagro Armenteros, Jesper Salomon, Henrik Nielsen, and Alexander Rosenberg Johansen. Netsolp: predicting protein solubility in escherichia coli using language models. *Bioinformatics*, 38(4):941–946, 2021.
- [34] Bin Li and Dengming Ming. Gatsol, an enhanced predictor of protein solubility through the synergy of 3d structure graph and large language modeling. *BMC Bioinformatics*, 25(1), 2024.